

Molecular Dynamics Study of the Stabilization of the Silica Hexamer $\text{Si}_6\text{O}_{15}^{6-}$ in Aqueous and Methanolic Solutions

S. Caratzoulas* and D. G. Vlachos

Department of Chemical Engineering, University of Delaware, Newark, Delaware 19716

Received: October 22, 2007; In Final Form: November 27, 2007

We use molecular dynamics simulations to study the stabilization of the hexameric, cage-like silicate with double three-ring structure in aqueous and methanolic solutions. We find that in purely aqueous environments its stabilization requires the presence of both tetramethylammonium and tetraethylammonium (TEA) cations and involves the formation of a stable TMA layer which leads to a water–silicate heteronetwork clathrate. We also find that TEA alone can facilitate stabilize the hexamer when methanol cosolvent is added, in accordance with experiment. The mechanism of this stabilization, however, differs from that in purely aqueous environments. Because of the unique properties of water–methanol mixtures, the organosilicate complex does not participate in heteronetwork clathrates but resides in a large solvent cavity; that is, it is forced out of true solution.

The role of organic cations (e.g., quaternary ammonium cations) in zeolite synthesis and crystallization remains enigmatic, and controversy surrounds aspects of their function. A fundamental question we would like an answer to is the following: do they act as templates that organize silicate clathrates around them,^{1–8} or do they act as external “scaffolds” that organize the solvent and stabilize the heteronetwork clathrates of oligosilicate hydrates?^{9–13} As many of the underpinning assumptions^{2,3,7,8} of the template model and of the structural fragment condensation theory for zeolite nucleation and growth are being refuted,^{10,14–19} we are still faced with the challenges of rationalizing the structures of the principal silicate anions that are found in aqueous alkaline solution, and of uncovering the influence of the organocations on silicate speciation.

The fact that different tetraalkylammonium (TAA) cations favor some species over others indicates that the organocations surely have a role in their preferential stabilization and, in terms of understanding the molecular level mechanism of zeolite formation, it is important to elucidate it. The physical or chemical mechanisms that control the nature of silicate hydrates of quaternary ammonium cations obviously also influence the nature of subcolloidal zeolite nanoparticle precursors.^{20–24} Thus, it is not unreasonable to expect that these mechanisms should also control zeolite evolution over longer time scales. In that respect, very useful supporting information may come from the study of these species, which structurally may be considered as host–guest systems (heteronetwork clathrates^{25–27}).

One of the most dramatic examples of silicate speciation is the case of the cage-like silicates Q_8^3 (cubic octamer) and Q_6^3 (prismatic hexamer). Q_8^3 is the dominant species in solutions prepared with TAA cations having alkyl group chain lengths of three or less. (The nanotechnological significance of these oligosilicate species is nicely demonstrated in the work of Laine and co-workers; e.g., see ref 28 and references therein.)

Using molecular dynamics simulations, we recently demonstrated that a strong correlation exists between the stability of Q_8^3 or Q_6^3 and their ability to support a full, stable layer of TMA^+ cations.^{11–13} That such a relation should exist had been hypothesized before but proved difficult to check experimentally.^{10,18} The claim has been that, because of the TAA cation's hydrophobic character, a layer of cations shields the cage-like polysilicate anions from the bulk solution, impeding hydrolysis.

Strong evidence in favor of the scaffold theory is also provided by the fact that small amounts of alkali-metal cations may accelerate zeolite nucleation and growth.^{18,29} Using molecular simulation, we recently demonstrated that the presence of sodium cations has an adverse effect on the silicate polyion– TMA^+ binding. This is a consequence of the sodium cations' ability to supplant the organic cations from silicate surfaces and weaken the clathrate structure hosting the polysilicate, facilitating further polymerization and growth. As the sodium counterions settle around the octamer, they polarize the local solvent and, as a result, disrupt the local water–water H-bond network by causing a substantial drop in the fraction of four-bonded water molecules. Eventually, a TMA cation relinquishes its position at the surface of the octamer, because the organocation—which itself induces higher water ordering in its vicinity—cannot be accommodated by the highly polarized environment.¹³

What emerges is that, altogether, the organocations play a significant role in reorganizing the solvent around the cage-like silicates in a manner conducive to the formation of heteronetwork clathrates that are stable both thermodynamically and kinetically. Transient species—that may indeed form but participate in floppy clathrates—eventually have to give way to cage-like polysilicates that lead to more rigid structures, like the octamer.¹⁰

The prismatic hexamer may be a transient species in aqueous TMA solution, but it is a stable species, nonetheless; single crystals of $(\text{NEt}_4)_6[\text{Si}_6\text{O}_{15}]\cdot 40.8\text{H}_2\text{O}$ have been studied by Wiebcke and Felsche using low-temperature X-ray diffraction.²⁷

* Author to whom correspondence should be addressed. E-mail: cstavros@udel.edu.

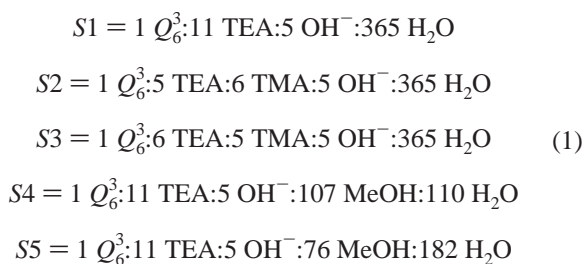
TABLE 1: Intermolecular Force Field Parameters for Pairwise-Additive Potentials between Atomic Sites

atom	ϵ^a (kcal/mol)	σ^a (Å)	q^b
Water			
O	0.1521	3.1501	-0.834
H	0.0	0.0	0.417
Tetramethylammonium (TMA)			
N	0.17	3.25	0.289
C	0.12	3.29	-0.302
H	0.02	1.78	0.160
Tetraethylammonium (TEA) ^c			
N	0.17	3.25	0.063
C ₁	0.118	3.905	0.21
C ₂	0.16	3.91	0.02
Silica Hexamer (Si ₆ O ₁₅ ⁶⁻) ^d			
Si	0.402	4.295	1.77
O _b	0.06	3.5	-1.04
O _t	0.06	3.5	-1.22

^a Lennard-Jones (6-12); $u(r) = 4\epsilon[(\sigma/r)^6 - (\sigma/r)^{12}]$. ^b Partial charges. ^c C₁ and C₂ denote CH₂ and CH₃, respectively, in the united atom representation. ^d O_b = siloxane, bridge oxygen; O_t = silanol, terminal oxygen.

In solution, however, NMR studies have shown that tetraethylammonium (TEA) alone cannot stabilize the hexamer; in fact, its stabilization requires a good deal of “coersion”, namely, both TEA and TMA, or a cosolvent, for example, methyl alcohol. For fixed, total [TEA + TMA] concentration and varying TEA mole fraction, x_{TEA} , Q_6^3 is the abundant species for $x_{\text{TEA}} \approx 0.5$.^{10,14,15,18,30,31}

A question, therefore, that arises is whether the purported correlation between stability and hydrophobic hydration (i.e., the protective shield hypothesis) holds true in the case of the hexamer, too. Admittedly, this has proven more of a challenge and has required a more deliberate approach for an unambiguous picture to emerge. We have performed molecular dynamics simulations in the following five systems:



In this Letter, we show that, in aqueous solutions, TEA alone, even at high concentrations, cannot form a stable layer around the prismatic hexamer; this is consistent with the aforementioned NMR observations. In fact, our simulations reveal a slightly more interesting situation: that in aqueous solution of TEA and TMA in almost equal amounts, and at room temperature, the TEA still cannot coordinate around the hexamer; only the TMA can—even though the latter is not always possible, and depends on the TEA-to-TMA ratio in the solution. However, when methanol cosolvent is added, then the TEA cations exhibit a remarkable ability to coordinate around the hexameric cage, with concomitant water exclusion; the molecular populations in *S4* and *S5* correspond to ~ 70 and 50% v/v methanol in water, respectively.

The force field parameters used in this study are given in Tables 1 and 2. Details on the force field parametrization and the partial charges, in particular, have been published elsewhere.^{11–13}

TABLE 2: Intramolecular Potential Parameters for TEA

Bond Angle ^a			
	k_a (kcal/(mol rad ²))	θ_0 (deg)	
C ₁ –N–C ₁ ^c	106.0	50.0	
N–C ₁ –C ₂	116.5	67.7	
Dihedral Angle ^b			
	A (kcal/mol)	δ (deg)	n
C ₁ –N–C ₁ –C ₂ ^c	0.10	0.0	3

^a $V_a(\theta) = (1/2)k_a(\theta - \theta_0)^2$. ^b $V_d(\phi) = A[1 + \cos(n\phi + \delta)]$. ^c C₁ and C₂ denote CH₂ and CH₃, respectively, in the united atom representation.

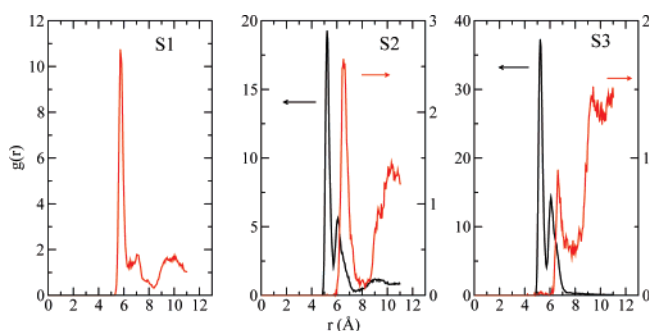


Figure 1. Hexamer–TMA (black line) and hexamer–TEA (red line) molecular-center distribution functions for the three systems S1–S3. In S2 and S3, the red lines are drawn on the right-hand scales.

All of the simulations were carried out in the canonical ensemble at 300 K using a Nosé–Hoover thermostat and Ewald summation for the electrostatics. Cubic periodic boundary conditions were employed with a lattice constant of 22.174 Å. The molecular populations of the simulation box are given in eq 1.

A few words on how the systems were prepared are in order. In system S1, each of 5 TEAs was placed opposite a face of the prismatic hexamer and each of the remaining 6 was placed opposite a terminal, silanol oxygen and along the Si–O[−] bond. The system was subsequently minimized in the gas phase, and the whole complex was submerged in water. Then, another round of minimization followed, to take care of accidental overlaps. A similar procedure was followed for systems S2 and S3; that is, the TEAs were placed opposite the faces of the hexamer in S2, and swapped positions with the TMAs in S3. Systems S1 and S2 were evolved for 1.5 ns, and system S3 was evolved for 2.0 ns. Systems S4 and S5 were prepared from S1 by substituting methanol for water in the simulation box. With the solute molecules held fixed in the simulation box, the systems were first equilibrated at 500 K for 50 ps, to accelerate the methanol–water mixing and then cooled down to the simulation temperature (300 K) with another 50 ps equilibration cycle. With the solute molecules then released, the systems were further equilibrated for 100 ps and then evolved for 1.5 ns, the observation period.

In Figure 1, we show the hexamer–TMA and hexamer–TEA molecular radial distribution functions (MRDFs) as functions of the separation of the molecular centers, for the three systems S1–S3. In S1, the near-neighbor peak of the Q_6^3 –TEA MRDF corresponds to 2 TEAs within 6.4 Å from the hexamer’s center of mass. Despite the high TEA concentration (1.7 M) and initial placement, the organocations quickly peel off the surface of the cage silicate, at room temperature. The TEA cations are forced off the surface by water molecules which move toward it and form a heteronetwork clathrate, which is supported via hydrogen bonds.

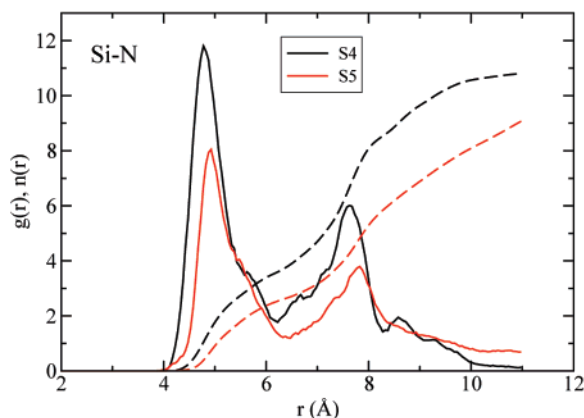


Figure 2. Si–N radial distribution functions in the systems S4 (black line) and S5 (red line). The dashed lines depict the corresponding running coordination numbers.

In S2, where TEA is pitted against TMA, neither one forms a layer around the hexamer. Moreover, TEA desorption is more favorable than in S1. From the Q_6^3 –TEA MRDF (Figure 1, panel S2, red line), we see that the TEAs are located farther away from the surface than in S1, and there are, on average, less than 0.5 TEAs within a radius of 8.0 Å from the hexamer’s molecular center. The two peaks in the Q_6^3 –TMA MRDF (panel S2, black line) correspond to coordination at the four-ring (primary peak) and three-ring faces; cations at the three-ring faces sit a bit farther away with respect to the hexamer’s center. In S2, the total number of TMAs (~ 2.7) at the surface is consistent with that obtained in previous studies with only TMA in solution.¹²

In system S3, where we have a 5:6 TMA-to-TEA ratio, we observe a rather dramatic turn in behavior: a stable TMA layer can now form around the hexamer. The Q_6 –TMA MRDF (cf. Figure 1, panel S3, black line) is similar in structure to that in S2, but the amplitudes are higher. As a result, we find 4.6 TMA cations at the surface of the silicate, 2.4 of which correspond to the primary peak. (For a representative configuration, see the image in Figure S1 in the Supporting Information.) This departure from the behavior of system S2 (where we have a 6:5 TMA-to-TEA ratio) is somehow unexpected. One could be tempted to rationalize it on the basis of electrostatics. Each methyl group in TMA carries more positive charge than in TEA (about 9 times as much, cf. Table 1), and therefore, TMA carries higher surface charge density. Thus, it is plausible that having the 5 TMA cations opposite the faces of the hexamer leads to more effective charge stabilization. Although there is nothing wrong with this argument, per se, it alone cannot explain why TMA does not stabilize the hexamer by itself. Other factors, such as geometry, should also be important.

The most compelling evidence in favor of the protective shield hypothesis and the scaffold theory is provided when methanol is added to the solution (systems S4 and S5). Then, the TEA cations exhibit a remarkable ability to coordinate around the hexameric cage, with concomitant water exclusion. In Figure 2, we show the Si–N RDF and corresponding running coordination numbers, in systems S4 (black lines) and S5 (red lines). Analysis shows that, in S4, there are, on average, 6 near-neighbor TEAs around the hexamer (3.6 of those are opposite four-ring faces); in S5, the coordination number drops to 4.5, with 2.7 TEAs opposite four-ring faces. Also, the layer of second-neighbor TEAs is more organized in S4 than in S5. (For a representative configuration, see the image in Figure S2 in the Supporting Information.)

TABLE 3: Number of Hydrogen Bonds Per Water or Methanol Molecule and the Statistical Estimate of the Expectation of the Number of Hydrogen Bonds per Molecule Present in the Methanol–Water Mixture

system	H-bonds per H ₂ O		H-bonds per MeOH		expectation per molecule
	H ₂ O–H ₂ O	H ₂ O–MeOH	MeOH–MeOH	MeOH–H ₂ O	
MethWat	2.0	1.4	0.8	1.3	2.8
S4	1.9	1.1	0.8	1.1	2.5
S5	2.4	0.7	0.4	1.7	2.8

In S4, from the hexamer–water MRDF, we find that only ~ 8 water molecules are coordinated in the immediate vicinity of the hexamer, forming hydrogen bonds with the silicate’s terminal oxygen atoms. This is in stark contrast both with the systems S1–S3, where we have ~ 35 waters around the hexamer, and with findings of earlier studies on the stabilization of the cubic octamer in aqueous solution of TMA.^{11–13} Thus, the organosilicate “complex” occupies a large cavity in the methanol–water solution. In S5, however, there are ~ 22 water molecules in the immediate vicinity of the hexamer, which signifies the dependence of the cavity formation on the methanol concentration in the solution. Furthermore, from the hexamer–methanol MRDF, ~ 4 methanol molecules are found close to the hexamer in S4, and zero in S5.

It is of interest to analyze the solvent structure in the methanolic solution and thereby understand the reasons for which the addition of methanol has such positive, stabilizing effects on the organosilicate complex. To investigate these matters, we have performed a detailed determination of the methanol–methanol, methanol–water, and water–water correlations both in systems S4 and S5 and in a system with the same water-to-methanol molecular ratio as in S4, but without the silicate and TEA solutes (hereinafter, this system will be referred to as MethWat). In particular, we have focused on the hydrogen-bond network of the methanol–water mixture.

Hydrogen bonding is manifested in several RDFs of water and methanol: OH, OH_w, and HO_w for hydrogen bonds involving methanol molecules and O_wH_w, O_wH, and H_wO for hydrogen bonds involving water molecules. (O and H denote the methanol hydroxyl group’s oxygen and hydrogen atoms; O_w and H_w are water’s oxygen and hydrogen atoms.) The degree of hydrogen bonding is estimated by calculating coordination numbers by integrating out to the first minimum to the right of the near-neighbor peak in the relevant site–site RDF. The results are summarized in Table 3.

In the system MethWat, this analysis gives ~ 0.8 methanol–methanol hydrogen bonds per methanol molecule, which is $\sim 56\%$ less than in pure methanol, and ~ 2.0 water–water hydrogen bonds per water molecule, which is $\sim 46\%$ fewer than in pure water. In addition, for each methanol molecule present in the MethWat mixture, we have ~ 1.3 hydrogen bonds between methanol and water, and for each water molecule in the mixture, we also estimate ~ 1.4 hydrogen bonds to methanol molecules. Overall, we have ~ 2.1 hydrogen bonds per methanol molecule—that is, the methanol–water H-bonds more than make up for the lack of the methanol–methanol ones—and ~ 3.4 per water molecule—only an 8% deficit with respect to pure water. The statistical estimate of the expectation of the number of hydrogen bonds per molecule present in the MethWat mixture is ~ 2.8 .

In system S4, the water–water and water–methanol H-bonds slightly drop (cf. Table 3) and the statistical estimate of the expectation of the number of hydrogen bonds per solvent molecule drops to ~ 2.5 —about 10% fewer than in MethWat. The H-bond deficit in S4 relative to MethWat should be

attributed to the formation of the cavity that accommodates the organosilicate and the concomitant geometry restrictions imposed upon the solvation molecules.

Therefore, one notable conclusion is that the methanolic solvent structure is practically the same in the two systems and rather unaffected by the presence of the solute molecules (i.e., hexamer and TEA). The two solvents reorganize to establish an H-bond network which results in negative entropy of mixing. (The average number of H-bonds per molecule for a methanol–water system of the same composition as in MethWat that have not yet been mixed is ~ 1.4 .)

Thus, in methanolic solutions, the solvent plays a different role from that in purely aqueous environments. In the latter, the solvent actively participates in the formation of heteronetwork clathrates, as in a host–guest system.^{11–13} In the former, we find the water molecules to prefer to associate with methanol rather than the silicate solute. As a result, the organosilicate complex occupies a large solvent cavity, with very few water molecules and no methanol molecules in the immediate vicinity of the polyion. Thus, it appears that the solubility of the organosilicate complexes in methanolic solution is such that they are forced out of true solution and may occur as large particles, perhaps of colloidal dimensions.

One very important question must be addressed, however. Is what we see in systems S4 and S5 the result of merely diluting the solution with methanol, and would we, therefore, observe the same effects irrespective of the presence of the TEA cations? The answer is no; the presence of TEA is extremely important. We have simulated the system S6 = 1 Q_6^{3+} :6 Na^+ :107 MeOH:110 H_2O where we have kept the same water-to-methanol molecular ratio as in S4 but removed the TEA cations; for electroneutrality, we have added 6 sodium cations. In the absence of TEA and with the sodium cations on the surface of the silicate polyion, the water molecules swiftly surround the hexamer and re-establish their H-bonds with the terminal oxygen atoms. On average, there are ~ 3.0 near-neighbor water molecules per Q_6^3 terminal oxygen in S6, whereas there are only ~ 1.0 in S4.

We have shown, in accordance with experiment, that the stabilization of the prismatic hexamer in aqueous solution requires the presence of TMA in addition to TEA. TMA alone, as we have shown in previous studies, cannot do the job, no matter how high its concentration. Finally, we have shown that TEA alone can facilitate stabilize the hexamer when methanol cosolvent is added, in accordance with experiment. The mechanism of this stabilization, however, differs from that in purely aqueous environments. Because of the unique properties of water–methanol mixtures, the stable organosilicate does not participate in heteronetwork clathrates but resides in a large solvent cavity; that is, it is forced out of true solution. We are currently investigating the effects of higher alcohols.

Acknowledgment. This work was supported in part by the US Department of Energy (DE-FG02-05ER25702).

Supporting Information Available: In Figure S1, we show a representative configuration in the immediate vicinity of the hexamer for system S3. In Figure S2, we show a representative configuration in the immediate vicinity of the hexamer for system S4. (All images were rendered using VMD.) This material is available free of charge via the Internet at <http://pubs.acs.org>.

References and Notes

- (1) Chang, C. D.; Bell, A. T. *Catal. Lett.* **1991**, *8*, 305–316.
- (2) den Ouden, C.; Datema, K.; Visser, F.; Mackay, M.; Post, M. *Zeolites* **1991**, *11*, 418–424.
- (3) de vos Burchart, E.; Jansen, J.; van der Graaf, B.; van Bekkum, H. *Zeolites* **1993**, *13*, 216.
- (4) Burkett, S. L.; Davis, M. E. *J. Phys. Chem.* **1994**, *98*, 4647–4653.
- (5) Burkett, S. L.; Davis, M. E. *Chem. Mater.* **1995**, *7*, 920–928.
- (6) Burkett, S. L.; Davis, M. E. *Chem. Mater.* **1995**, *7*, 1453–1463.
- (7) Lewis, D.; Willock, D.; Catlow, C.; Thomas, J. M.; Hutchings, G. *Nature* **1996**, *382*, 604.
- (8) Wu, M.; Deem, M. J. *Chem. Phys.* **2004**, *116*, 2125.
- (9) Kinrade, S.; Pole, D. *Inorg. Chem.* **1992**, *31*, 4558.
- (10) Kinrade, S. D.; Knight, C. T. G.; Pole, D. L.; Syvitski, R. *Inorg. Chem.* **1998**, *37*, 4278–4283.
- (11) Caratzoulas, S.; Vlachos, D.; Tsapatsis, M. *J. Phys. Chem. B* **2005**, *109*, 10429.
- (12) Caratzoulas, S.; Vlachos, D.; Tsapatsis, M. *J. Am. Chem. Soc.* **2006**, *128*, 596–606.
- (13) Caratzoulas, S.; Vlachos, D.; Tsapatsis, M. *J. Am. Chem. Soc.* **2006**, *128*, 16138.
- (14) Harris, R. K.; Knight, C. T. G. *J. Chem. Soc., Faraday Trans. 2* **1983**, *79*, 1525.
- (15) Harris, R. K.; Knight, C. T. G. *J. Chem. Soc., Faraday Trans. 2* **1983**, *79*, 1539.
- (16) Knight, C. J. *Chem. Soc., Dalton Trans.* **1988**, 1457.
- (17) Kinrade, S.; Swaddle, T. *Inorg. Chem.* **1988**, *27*, 4259.
- (18) Kinrade, S. D.; Knight, C. T. G.; Pole, D. L.; Syvitski, R. *Inorg. Chem.* **1998**, *37*, 4272–4277.
- (19) Knight, C.; Kinrade, S. J. *Phys. Chem. B* **2002**, *106*, 3329.
- (20) Fedeyko, J. M.; Rimer, J. D.; Lobo, R. F.; Vlachos, D. G. *J. Phys. Chem. B* **2004**, *108*, 12271–12275.
- (21) Fedeyko, J.; Sawant, K.; Kragten, D.; Vlachos, D.; Lobo, R. *Stud. Surf. Sci. Catal.* **2004**, *154*, 1267–1273.
- (22) Fedeyko, J.; Vlachos, D.; Lobo, R. *Langmuir* **2005**, *21*, 5197–5206.
- (23) Rimer, J.; Vlachos, D.; Lobo, R. F. *J. Phys. Chem. B* **2005**, *109*, 12762–12771.
- (24) Rimer, J.; Lobo, R.; Vlachos, D. *Langmuir* **2005**, *21*, 8960–8971.
- (25) Wiebcke, M.; Hoebbel, D. *J. Chem. Soc., Dalton Trans.* **1992**, 2451–2455.
- (26) Wiebcke, M.; Grube, M.; Koller, H.; Engelhardt, G.; Felsche, J. *Microporous Mater.* **1993**, *2*, 55–63.
- (27) Wiebcke, M.; Felsche, J. *Microporous Mesoporous Mater.* **2001**, *43*, 289–297.
- (28) Laine, R. J. *Mater. Chem.* **2005**, *15*, 3725–3744.
- (29) Kumar, R.; Bhaumik, A.; Ahedi, R.; Ganapathy, S. *Nature* **1998**, *381*, 298.
- (30) Knight, C. T. G.; Kirkpatrick, R. J.; Oldfield, E. J. *J. Am. Chem. Soc.* **1986**, *108*, 30.
- (31) Knight, C. T. G.; Kirkpatrick, R. J.; Oldfield, E. J. *J. Am. Chem. Soc.* **1987**, *109*, 1632.